Title

Theta Oscillations Index Frontal Decision-Making and Mediate Reciprocal Frontal–Parietal Interactions in Willed Attention

Journal

Cerebral Cortex, 29(7)

ISSN

1047-3211

Authors

Rajan, Abhijit
Siegel, Scott N
Liu, Yuelu
et al.

Publication Date

2019-07-05

DOI

10.1093/cercor/bhy149

Peer reviewed

Cerebral Cortex, July 2019; 2832–2843

doi: 10.1093/cercor/bhy149
Advance Access Publication Date: 21 June 2018
Original Article

ORIGINAL ARTICLE

Theta Oscillations Index Frontal Decision-Making and Mediate Reciprocal Frontal–Parietal Interactions in Willed Attention

Abhijit Rajan[1], Scott N. Siegel[1], Yuelu Liu[2], Jesse Bengson[3], George R. Mangun[2,4] and Mingzhou Ding[1]

[1]J. Crayton Pruitt Family Department of Biomedical Engineering, University of Florida, Gainesville, FL 32611, USA, [2]Center for Mind and Brain, University of California, Davis, CA 95618, USA, [3]Department of Psychology, Sonoma State University, Rohnert Park, CA 94928, USA and [4]Departments of Psychology and Neurology, University of California, Davis, CA 95616, USA

Address correspondence to Mingzhou Ding. Email: mding@bme.ufl.edu

Abstract

Attention can be attracted reflexively by sensory signals, biased by learning or reward, or focused voluntarily based on momentary goals. When voluntary attention is focused by purely internal decision processes (will), rather than instructions via external cues, we call this "willed attention." In prior work, we reported ERP and fMRI correlates of willed spatial attention in trial-by-trial cuing tasks. Here we further investigated the oscillatory mechanisms of willed attention by contrasting the event-related EEG spectrogram between instructional and choice cues. Two experiments were conducted at 2 different sites using the same visuospatial attention paradigm. Consistent between the 2 experiments, we found increases in frontal theta power (starting at ~500 ms post cue) for willed attention relative to instructed attention. This frontal theta increase was accompanied by increased frontal–parietal theta-band coherence and bidirectional Granger causality. Additionally, the onset of attention-related posterior alpha power lateralization was delayed in willed attention relative to instructed attention, and the amount of delay was related to the timing of frontal theta increase. These results, replicated across 2 experiments, suggest that theta oscillations are the neuronal signals indexing decision-making in the frontal cortex, and mediating reciprocal communications between the frontal executive and parietal attentional control regions during willed attention.

Key words: alpha lateralization, coherence, EEG, GC, visuospatial attention

Introduction

The ability to focus attention on relevant events in the environment and avoid distraction is at the core of perception and performance. The mechanisms of voluntary attention have been extensively studied using cuing paradigms in which a cue instructs the subject to pay attention to a task-relevant class of stimuli, based, for example, on spatial location or object properties (Posner 1980). For voluntary visual spatial attention, cues that direct attention to relevant locations in the visual field lead to improved speed and accuracy in target stimulus processing at cued (attended) location (Posner 1978; Carrasco 2011), larger sensory event-related potentials (Voorhis and Hillyard 1977; Mangun and Hillyard 1991), increased firing rates of visual neurons (Moran and Desimone 1985; Reynolds and Chelazzi 2004), and larger hemodynamic activities (Heinze et al. 1994, Tootell et al. 1998; Hopfinger et al. 2000).

Mechanisms of attentional control can be revealed by investigating brain activity in the period following a cue that directs attention but before the appearance of the task-relevant targets or irrelevant distractors. A highly reproducible neuroimaging finding is that following an attention-directing cue, the dorsal attention network (DAN), including bilateral frontal eye fields (FEF) and bilateral intraparietal sulcus (IPS), is activated and serves to implement the attentional set and to issue signals to bias sensory processing (Kastner et al. 1999; Hopfinger et al. 2000; Corbetta and Shulman 2002; Giesbrecht et al. 2003; Bressler et al. 2008; Wen et al. 2012; Liu et al. 2016; Wang et al. 2016). Hence, the activation of the DAN is correlated with the allocation of voluntary attention in response to the external cue that directs the focus of attention.

In naturalistic settings, however, attention is often directed to aspects of the environment according to purely internally generated goals and decisions, rather than goals imposed externally by cues. Recent work has attempted to broaden the scope of the classic cuing paradigm by incorporating a new type of trial where the subject is asked to decide for themselves where to allocate spatial attention. For example, in addition to instructional cues presented at the beginning of a trial, Taylor et al. (2008) included what they called choice cues where the subjects could use their free will to select where to attend on that trial, among several equal alternatives; we have termed the ensuing behavior willed attention (Bengson et al. 2014), derived from related studies of willed action (Lau et al. 2004). FMRI studies of willed attention have identified a set of brain regions in medial frontal, lateral frontal and inferior parietal cortices that are more active for choice cues relative to instructive cues (Taylor et al. 2008; Bengson et al. 2015; Liu et al. 2017). An EEG study has further isolated choice cue-specific ERP components in the frontal and central parietal regions, occurring 250–350 and 400–800 ms, respectively, after the cue onset (Bengson et al. 2015), and related work has identified precue oscillatory activity in the EEG that predicted where subjects would choose to attend on a trial-by-trial basis (Bengson et al. 2014).

In a recent report, Liu et al. (2017) applied graph theoretic techniques to fMRI data from a willed attention paradigm, and showed that spontaneous decisions of where to attend are computed in the frontal regions, and then communicated to the parietal cortex for the attentional set to be implemented. Here we investigate the neuronal signals and the temporal dynamics of the neuronal signals mediating such frontal–parietal interactions. The technique of fMRI, owing to its non-neural nature and poor temporal resolution, has limited ability to address this problem, and hence we turn to the investigation of EEG oscillatory activity in the postcue/pretarget interval.

In diverse tasks requiring "top-down" processing, such as working memory (Sauseng et al. 2005), cognitive control (Gulbinaite et al. 2014), and preparatory attention (Sauseng et al. 2008), long-range communications between distant brain regions are found to be mediated through theta-band neuronal oscillations (3–7 Hz) (von Stein and Sarnthein 2000). The potential relevance of EEG theta in willed attention is further heightened by the fact that choosing among competing alternatives involves conflict resolution (Taylor et al. 2008; Walsh et al. 2011; Bengson et al. 2015; Liu et al. 2017) and frontal theta oscillations have a demonstrated role in conflict processing (Cohen and Donner 2013; Cavanagh and Frank 2014; Cohen 2014). In addition, as discussed earlier, frontal choice of attentional focus needs to be communicated to parietal attentional control regions for implementation, and theta oscillations have been implicated in frontal–parietal interactions (Sauseng et al. 2008). These considerations lead to the hypothesis that choice cues should be associated with higher frontal theta power, as well as higher frontal–parietal theta-band functional interactions. The goal of this study is to test this hypothesis.

To investigate the role of EEG theta in willed attention and test the replicability of the findings, we analyzed EEG and fMRI data from 2 cohorts of subjects recorded at 2 different sites (University of Florida and University of California at Davis), who performed the same willed attention task. Event-related EEG spectra were contrasted between the instructional cues and choice cues to identify the oscillatory activity specific to willed attention. Coherence and nonparametric Granger causality (GC) (Dhamala et al. 2008) were then applied to compare the strength and directionality of frontal–parietal communications during willed and instructed attention. In addition, we assessed the temporal dynamics of willed versus instructed attention by comparing the time courses of attention-related lateralization of posterior alpha (8–12 Hz) for each. Finally, correlating trial-by-trial oscillatory activity with the BOLD signals allowed us to elucidate the neuroanatomical substrates of willed attention-related EEG dynamics.

Materials and Methods

Overview

Two experiments were conducted, one at the University of Florida (UF) and the other at the University of California at Davis (UCD), using the same willed visual spatial attention paradigm. At UF, EEG, and fMRI were recorded simultaneously, whereas at UCD, EEG, and fMRI were recorded from the same subjects in separate sessions. Except for the minor differences in procedures noted below, the procedures and the methods were common between the 2 sites.

We note that separate analyses of these datasets, focused on different aspects of the data, have been published previously (Bengson et al. 2014, 2015; Liu et al. 2017). Specifically, Bengson et al. (2014) considered alpha oscillations before cue onset in the UCD dataset, Bengson et al. (2015) investigated ERPs and fMRI BOLD activity in the UCD dataset, and Liu et al. (2017) examined the fMRI data in both the UF and UCD datasets. Here, we focus on EEG oscillatory activity in the postcue/pretarget period, during which decisions about where to attend in the willed attention condition are being made, and voluntary spatial attention is being allocated and maintained.

Participants

UF: The experimental protocol was approved by the Institutional Review Board of the University of Florida. A total of 18 right-handed subjects with normal or corrected to normal vision and no history of neurological or psychological disorders gave written informed consent and took part in the experiment. Data from 5 participants were excluded from the analysis based on the following reasons: 1) behavioral performance was below criterion (<70% accuracy, 1 participant); 2) unable to follow the task instructions (1 participant); and 3) excessive body or eye movements in the scanner (3 participants). For one additional subject, due to equipment malfunctioning, there was a mismatch in the event triggers between fMRI and EEG data; this subject was used in the EEG-only and fMRI-only analysis but not in the EEG-informed fMRI analysis.

UCD: The experimental protocol was approved by the Institutional Review Board of the University of California at

Davis. Overall, 18 right-handed subjects with normal or corrected to normal vision and no history of neurological or psychological disorders gave written informed consent and took part in the experiment (Bengson et al. 2015). One subject was rejected from fMRI data analysis for failure to follow instructions during the fMRI session.

Paradigm and Procedure

As illustrated in Figure 1, each trial began with one of 3 symbolic cues (circle, square or triangle) displayed slightly above the central fixation for a duration of 200 ms. Two of the cues, called instructional cues, directed the subject to covertly direct their attention to the left or right visual field while the third, the choice cue, directed the subject to choose the side of the visual field to attend on that trial. The 3 cue conditions occurred with equal probability and the meanings of the 3 shapes used as symbolic cues were counterbalanced across subjects. Following a variable cue-target interval (stimulus-onset asynchrony or SOA) of 2000–8000 ms, a black and white grating appeared in one of the visual hemifields for a duration of 100 ms; for all trials the targets were equally likely to be on the left or right, and for the instructional cue trials, the cue matched the target side 50% of the time (i.e., the cues were not predictive). The subject's task was to discriminate the spatial frequency of the stimulus (0.2° per cycle vs. 0.18° per cycle for UCD dataset; 0.53° per cycle vs. 0.59° per cycle for UCD dataset) appearing in the attended hemifield with a button press and ignore the stimulus appearing in the unattended hemifield. Subjects were instructed to respond as fast and accurately as possible. Following a variable interstimulus interval (SOA) of 2000–8000 ms, the participants were prompted by the visual cue "?SIDE?" to report which side they were attending on that trial via a button press. A variable intertrial interval (SOA) of 2000–8000 ms followed the side report cue. This task was designed using the Presentation® software (www.neurobs.com).

The present paradigm differs from the Posner style paradigms using probabilistic cuing of target location to manipulate spatial attention (Posner 1980), which require responses to stimuli in both the attended (cued) and the unattended (uncued) visual hemifield. In our paradigm, instructional cues direct the subject where to focus 100% of their attention on each trial, and because subjects focused spatial attention fully, there should be minimal spread of attention toward the unattended location; the same was true for the choice cue trials where the subjects were told that when they picked a side to attend, they should allocate 100% attention to that side. Although the cue-target is relatively long to accommodate the sluggish BOLD response, the high perceptual load of the target discrimination task encouraged the focused allocation and maintenance of covert attention towards the instructed or chosen hemifields (Handy and Mangun 2000). In addition, a pilot experiment using the standard probabilistic Posner cueing paradigm with the same stimulus presentation scheme and task parameters was also conducted, and the behavioral results of this pilot experiment clearly showed that subjects responded faster for validly cued targets as compared with the invalidly cued targets and that the effects do not differ significantly between instructed and choice cue conditions (Bengson et al. 2014).

Prior to recording, all participants completed a training session to ensure stable performance to criterion (above 70% accuracy on the spatial frequency discrimination, and close to 0% errors in responding to uncued-location targets).

Data Acquisition

UF fMRI: Functional magnetic resonance images were obtained on a 3 T Philips Achieve Scanner equipped with a 32-channel head coil. The echo planar sequence (EPI) had the following parameters: repetition time (TR) = 1980 ms; echo time = 30 ms;

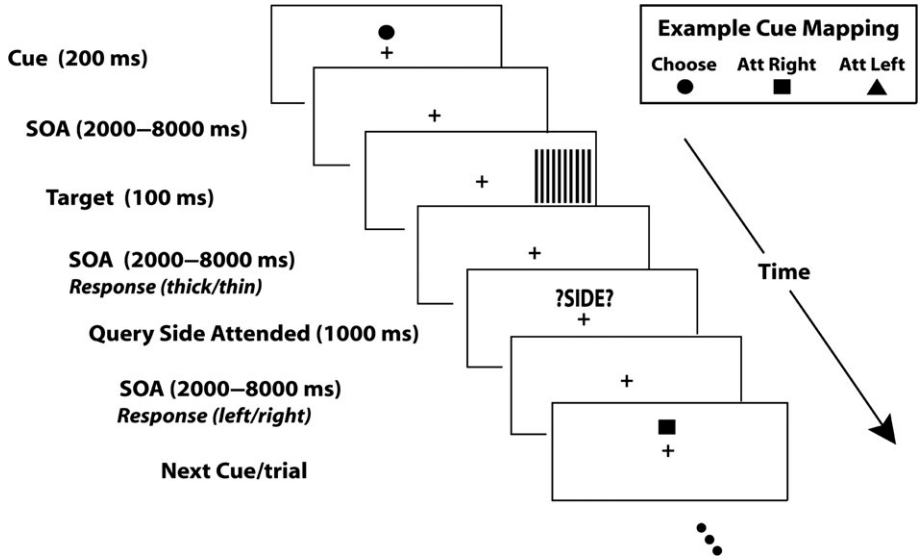

Figure 1. Schematic of the trial-by-trial cuing paradigm. Each trial started with a visual symbolic cue (200 ms) that either directed the subject to covertly attend to the left or the right hemifield, or to spontaneously choose which hemifield to covertly attend for that trial (an example cue mapping is shown at lower right; the mapping was counterbalanced across subjects). Following a variable stimulus onset asynchrony (SOA) from cue to target of 2000–8000 ms, a high-contrast grating target was flashed in either the left or right hemifield. Participants were asked to report the spatial frequency of the grating appearing in the attended hemifield, and to ignore the grating in the unattended hemifield (they responded with a button to indicate whether the grating lines appeared to be "thick" or "thin"). Following the target with an SOA of 2000–8000 ms, a visual prompt ("?SIDE?") was displayed, which prompted the subjects to report the attended spatial location (left or right) for that trial; this was required for all trials, regardless of whether the trial was an instructed or choice cue trials. The next trial began a random 2000–8000 ms after the onset of the "side" prompt.

flip angle = 80°; field of view = 224 mm; the number of axial slices = 36.

UF EEG: Continuous EEG data was recorded inside the MRI scanner simultaneously with fMRI using a MR-compatible 32-channel EEG acquisition system (Brain Products, Germany). In total, 31 electrodes were placed on the scalp based on the 10–20 system using an elastic cap. The remaining electrode was placed on the upper back near the spine to record the ECG signal, which was used subsequently to remove ballistocardiogram (BCG) artifacts (Ertl et al. 2010). The FCz channel was used as a reference during recording. The impedance of all scalp channels was kept under 5 kΩ. The sampling frequency was 5000 Hz.

UCD fMRI: Functional magnetic resonance images were obtained on a 3 T Siemens Skyra scanner with a 32-channel head coil. The EPI sequence had the following parameters: TR = 2100 ms; echo time = 30 ms; flip angle = 90°; field of view = 218 mm; the number of axial slices = 34.

UCD EEG: Continuous EEG data was recorded from 64 tin electrodes mounted in an elastic cap (Electro-cap International Inc., Eaton, Ohio) using Synaps2 amplifiers (Compumedics/Neuroscan, Charlotte, NC). The reference electrode was placed at the right mastoid during recording. The impedance of all scalp channels was kept below 5 kΩ. The sampling frequency was 1000 Hz.

Functional MRI Analysis

Preprocessing: The preprocessing of fMRI data was performed with SPM and included the following steps: slice time correction, motion realignment, spatial normalization and smoothing. The slice timing correction in SPM used sinc interpolation to account for the acquisition delay for each slice in a given EPI volume. Motion realignment was performed by coregistering all images with the first scan of each session. Six motion parameters (3 translational and 3 rotational) were calculated and entered into the design matrix to be regressed out in the general linear model (GLM) analysis. All images were spatially normalized to the standard MNI space and resampled to a voxel resolution of $3 \times 3 \times 3\,mm^3$. The spatially normalized images were smoothed using a Gaussian kernel of 8 mm full width at half maximum. A high-pass filter with a cut-off frequency of 1/128 Hz was used to remove any low frequency noise.

Cue-related BOLD activation: In the GLM, 7 regressors were used to model the relevant events in the task. Five of these regressor represented cue events, and 2 regressors represented stimulus events. Among the 5 cue-related regressors, 2 were for instructional cues (attend left and attend right), 2 for choice cues (choice left and choice right), and 1 for trials with incorrect responses in the discrimination of spatial frequency of the targets. The 2 stimulus regressors represented stimulus presentation in the left and right visual field, respectively. The individual level BOLD activation maps were obtained by contrasting the beta parameters associated with the appropriate regressors. The group level activation map was obtained by performing a one-sample *t*-test over the individual subject contrast maps (random-effects modeling). This group level activation map was false discovery rate (FDR) corrected ($P < 0.05$) to account for multiple comparisons.

EEG Analysis

Preprocessing: For the UF dataset, because EEG was recorded simultaneously with fMRI inside the scanner, extra steps were required to remove the MRI artifacts. Both gradient and BCG artifacts were removed using a template based artifact subtraction method implemented in the Brain Vision Analyzer software (Allen et al. 1998, 2000). Specifically, the gradient artifact was removed by constructing an average artifact template over 41 consecutive volumes in a sliding window fashion, and then subtracting this template from the raw EEG for each volume. For the BCG artifact removal, ECG R-waves were first detected, and 21 consecutive ECG segments defined around the R waves were averaged to produce a BCG artifact template. This template was then subtracted from the EEG to remove BCG contamination. After removing the MRI artifacts, the preprocessing and data analysis procedures for UF and UCD EEG datasets were the same, as follows.

EEG data was bandpass filtered between 0.1 and 50 Hz, and downsampled to 250 Hz. Further preprocessing was performed within EEGLAB. The continuous EEG data were epoched from 500 ms before to 1500 ms after the cue onset. Epochs were visually inspected for artifact contamination and trials with excessive muscle or body movement related artifact were removed. Trials with excessive eye movements or blinks were rejected. In UF dataset, the mean number of artifact-free trials for each subject were 133 for instructed attention condition and 67 for willed attention condition, per subject. In UCD dataset, the instructed attention condition had on average 165 artifact-free trials and the willed attention condition had on average 79 artifact-free trials, per subject. To remove the negative impact of volume conduction and common reference, the artifact-corrected scalp voltage data was converted to reference-free current source density (CSD), by calculating 2D surface Laplacian (Tenke and Kayser 2012). All further analysis including spectrogram and functional connectivity calculations were performed on the CSD data.

Time–frequency analysis: Time–frequency analysis was performed by calculating spectrograms using short-time Fourier transforms with moving windows of 500 ms in duration and 20 ms in step size. Each condition's spectrogram was normalized to its precue baseline activity (−500 to 0 ms). All the power spectral calculations were performed after subtracting the ensemble mean (ERP) of that condition from all trials, in order to minimize the influence of evoked response on the spectrum (Kalcher and Pfurtscheller 1995). This was done for each electrode, each condition and each subject separately. The statistical significance of the spectrogram difference between willed and instructed attention conditions was tested using a cluster-based permutation method (Maris and Oostenveld 2007). Specifically, within each permutation, the condition labels were randomly shuffled and a difference spectrogram ("willed" vs. "instructed") was computed. Each time–frequency pixel of the spectrogram was converted to a *t*-value. All pixels that survived $P < 0.05$ thresholding were clustered based on their temporal and spectral adjacency. The *t*-values within the cluster were summed (referred to as "mass") and used as a cluster level statistic. The maximum cluster level statistic (mass) was stored. After repeating this step 1000 times an empirical null distribution of the maximum cluster level statistic was obtained. The mass of a cluster from the actual data was compared with this null distribution and considered significant if $P < 0.05$.

Alpha lateralization analysis: In spatial attention, the power of posterior alpha oscillations is known to decrease over the visual cortex corresponding to the attended location, indicating a state of sensory readiness for processing attended information (Worden et al. 2000; Thut et al. 2006; Foster et al. 2017). Lateralization of posterior alpha oscillation is thus a reliable

index of covert visual spatial attention deployment. An alpha lateralization index (ALI) was defined as follows:

$$ALI = \frac{\alpha_{ipsi} - \alpha_{contra}}{\alpha_{ipsi} + \alpha_{contra}}$$

where, α_{ipsi} is the alpha power (8–12 Hz) averaged over the channels ipsilateral to the attended visual field and α_{contra} is the alpha power averaged over the channels contralateral to the attended visual field. For the left hemisphere, the channels were O1 and P3; for the right hemisphere, the channels were O2 and P4. Larger value of alpha lateralization indicates a stronger sensory bias towards the attended hemifield. The time course of alpha lateralization during a trial was calculated using the same moving window approach described above, where the statistical significance at each time point was tested by a one sample *t*-test, corrected for multiple comparisons by controlling the FDR. The earliest time point of the ALI time course where $P < 0.05$, FDR was considered to signify the beginning of sensory biasing, implemented by top-down control signals from the DAN.

EEG connectivity analysis: Interareal connectivity was assessed by computing spectral coherence and Granger causality between regions of interest (ROIs) (in the sensor space) over frontal and parietal regions using the Fourier method (Dhamala et al. 2008; Nedungadi et al. 2009). The frontal ROI comprised of adjacent central frontal channels Fz, F1, and F3, and the parietal ROI comprised the adjacent central parietal channels Pz, P1, and P3 (Fig. 2). The statistical significance of the difference in frontal–parietal coherence and Granger causality between willed and instructed conditions was assessed using paired *t*-tests.

Two comments are in order. First, we will use the shorthand of frontal–parietal here, but do not intend to imply that we have localized the signals to the intracranial neural sources; the small number of electrodes precluded a conclusive analysis in the source space. Second, to ensure that the unequal numbers of trials in willed and instructed conditions did not affect the connectivity results, we performed an additional analysis using a resampling technique, in which equal numbers of trials were drawn randomly from willed and instructed conditions multiple times to yield a willed ensemble and an instructed ensemble. The comparison of spectral quantities estimated from the 2 ensembles led to the same conclusions.

EEG-informed fMRI analysis: This analysis was only conducted for the UF dataset where the EEG and fMRI were recorded simultaneously. To examine the neuroanatomical substrate of the observed frontal EEG activity, separate regressors were added in the GLM to model the EEG–BOLD correlation. Specifically, in addition to the regressors described earlier, one additional parametric modulation based regressor (Büchel et al. 1998) containing the single-trial frontal theta power was added to the onset of each type of cue (attend left, attend right, choice left, choice right). For these regressors the height of the boxcar was multiplied with the single-trial frontal theta power. The beta coefficients obtained for these regressors indicate the strength of coupling between BOLD of a brain voxel and theta power modulation. For trials rejected during preprocessing because of artifacts, we substituted them with mean theta power calculated in the time period of interest for that condition. At the individual subject level a one sample *t*-test was performed on these beta coefficients to obtain the *t*-maps. At the group level, one sample test was performed on the individual subject *t*-map, and only voxels above a suitable threshold ($P < 0.05$) were reported in the final group level *t*-map.

Results

UF Dataset

Behavioral Analysis

The reaction time (RT) to the targets (i.e., discrimination of target spatial frequency) did not differ significantly between willed and instructed attention conditions (instructed attention: 910.95 ± 79.94 ms; willed attention: 929.03 ± 110.59 ms; $P > 0.05$). The accuracy also did not differ significantly between willed and instructed attention (76.48% and 82.10% for instructed and willed conditions, respectively, $P > 0.05$). These behavioral results suggest that participant's attention levels were approximately equated across willed and instructed attention conditions.

Cue-Related BOLD Activity

Previously, we have reported that higher target-evoked BOLD responses were observed for attended targets relative to the unattended targets, suggesting that the subjects sustained covert attention in the cue-target interval (Liu et al. 2017). The

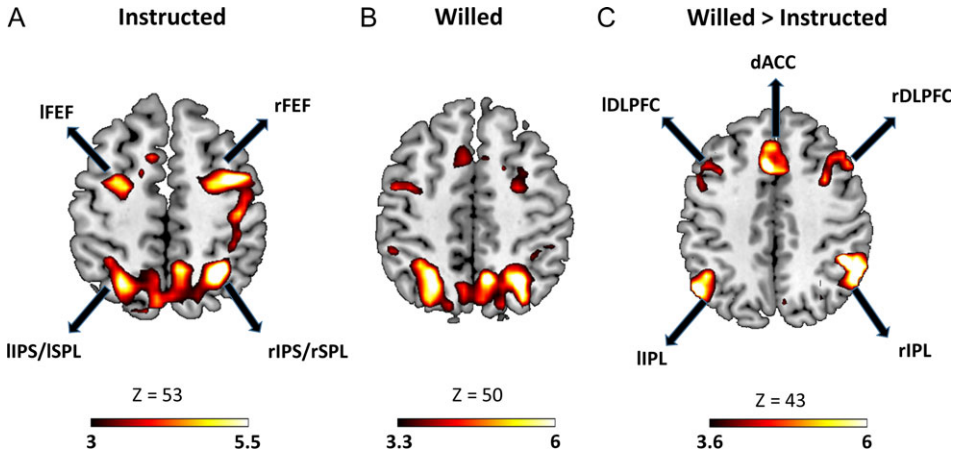

Figure 2. Significant BOLD activation ($P < 0.05$, FDR) evoked by (*A*) instruction cue and (*B*) choice cue. (*C*) Regions showing higher BOLD activity for choice cues as compared with instruction cues. lFEF, left frontal eye field; rFEF, right frontal eye field; lIPS, left intraparietal sulus; rIPS, right intraparietal sulcus; lSPL, left superior parietal lobule; rSPL, right superior parietal lobule; lSPL, left superior parietal lobule; lDLPC, left dorsolateral prefrontal cortex; rDLPFC, right dorsolateral prefrontal cortex, dACC, dorsal anterior cingulate cortex.

DAN was significantly activated in response to both willed and instructional cues (Fig. 2A,B), providing the neural basis of sustained spatial attention to the cued or chosen visual field. Contrasting willed against instructed attention revealed an additional network of frontal and parietal regions (Fig. 2C), including bilateral dorsolateral prefrontal cortex (DLPFC), bilateral anterior prefrontal cortex (APFC), superior frontal gyrus (SFG), inferior parietal lobule (IPL), presupplementary motor area (dACC/pre-SMA) and anterior insula, that are preferentially activated during willed condition (for more details on this result, please see Liu et al. 2017). The fact that DAN regions did not appear in the willed versus instructed contrast is taken to signify that the level of attention control was comparable between the 2 conditions, providing neural support for the behavioral results reported above, where no difference in RT and accuracy was seen between the 2 conditions.

Cue-Related EEG Oscillatory Activity

Increased frontal activations for willed relative to instructed attention are interpreted as being related to internally guided decision processes about where to attend (Taylor et al. 2008; Bengson et al. 2015; Liu et al. 2017), as well as in resolving the inherent conflict arising when deciding between 2 equal choices (Taylor et al. 2008; Walsh et al. 2011). To understand the neural underpinnings of these processes, and to relate the neuroanatomy to the neurophysiological signs of willed attention, we statistically compared frontal EEG spectrograms of willed attention and instructed attention (Fig. 3A). The statistically significant time–frequency difference cluster is shown in Figure 3B ($P < 0.05$, corrected for multiple comparisons via cluster-based permutation test). This analysis demonstrates that the frequency range of interest was in theta band (3–7 Hz), and the time period of interest was 400–800 ms after the onset of the cue. Based on the time frequency cluster, the onset and offset of this postcue theta power increase for willed versus instructed attention was calculated to be 470 and 690 ms post cue onset, respectively (Table 1). In addition, the frontal theta power was specifically compared between willed and instructed attention in the time period of interest, that is, 400–800 ms post cue, to find a significant increase during willed attention as compared with instructed attention ($P < 0.05$). The power spectral densities in the time period of interest are plotted for all frequencies in Figure 3C to further demonstrate the enhanced frontal theta oscillations in willed condition. The parietal region of interest showed no significant time frequency cluster in theta band for the willed attention as compared with the instructed attention (Fig. 3D,E). The parietal theta power was not significantly different between the willed and instructed condition in the time period 400–800 ms post cue ($P > 0.05$), which was demonstrated in the power spectral density plot in Figure 3F. This increase in theta power selectively in frontal channels is consistent with the BOLD findings, which showed that significant signal increases for willed versus instructed attention occurred primarily in frontal cortex.

EEG Functional Connectivity

The functional connectivity between frontal theta and parietal theta oscillatory activities was assessed by computing theta-band coherence between the frontal and parietal scalp electrode ROIs during the time period of interest (400–800 ms). As shown in Figure 4A, the frontal–parietal theta coherence was significantly higher for the willed condition as compared with the instructed condition ($P < 0.05$), lending support to our prior fMRI study asserting an important role of frontal–parietal interaction in willed attention (Liu et al. 2017). To decompose the frontal–parietal communication into its directional components, frontal→parietal, and parietal→frontal, we computed nonparametric Granger causality (GC) in the theta band. Figure 4B and C revealed that the willed condition had

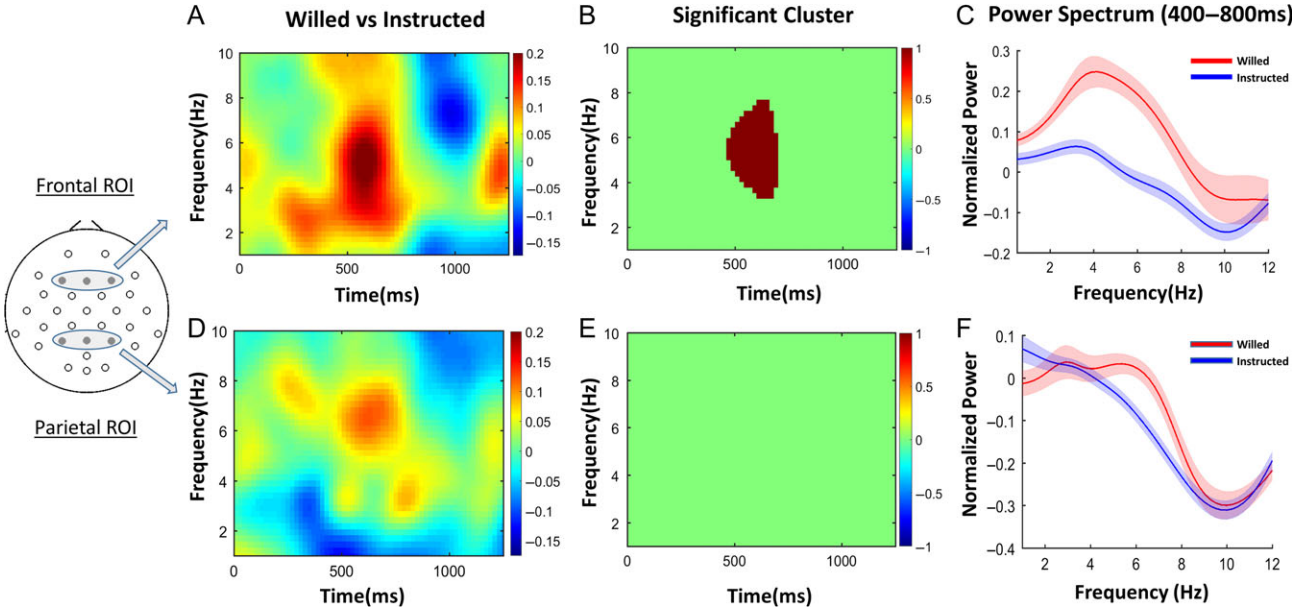

Figure 3. Spectral analysis of willed and instructed attention. (*A*) Cue evoked spectrogram averaged across frontal regions of interest (ROI; shown at left). (*B*) The time–frequency cluster showing significant difference between willed and instructional cues ($P < 0.05$, cluster-based permutation test). (*C*) The power spectral density in the time period of interest (400–800 ms) showing clear increase in theta power (3–7 Hz) for willed compared with instructed attention ($P < 0.05$). (*D*)–(*F*) The same analyses applied to the EEG recorded from the parietal region of interest. No time–frequency clusters were significantly different between the 2 conditions in the parietal ROI. There was no difference in the theta band power in the time period 400–800 ms ($P > 0.05$).

significantly higher GC in both directions as compared with the instructed condition (frontal→ parietal, $P < 0.05$; parietal → frontal, $P < 0.05$). Such enhanced bidirectional interaction suggests that in willed attention the frontal structures not only send information about where to attend to the parietal attention control regions but also receive input from these parietal regions about the current attentional state as part of the frontal cortex's monitoring function (Heekeren et al. 2008). A schematic illustration of the GC results is given in Figure 4D.

Time Course of Attention Allocation

In visual spatial attention, alpha power decreases over the posterior scalp contralateral to the attended visual hemifield (Thut et al. 2006; Rajagovindan and Ding 2011). Here, we used the alpha lateralization index (ALI) computed using a moving window approach to assess the time course of attentional set implementation in willed and instructed conditions. As shown in Figure 5C, the development of the spatial attention set was clearly delayed in the case of willed condition as compared with the instructed condition. Specifically, alpha lateralization became statistically significant ($P < 0.05$ FDR corrected) at 730 ms post cue and 1190 ms post cue for instructed and willed condition, respectively (Table 1). The 460 ms delay is likely attributable to the added frontal processing time of the choice cue. At 730 ms post cue, the alpha power topographic maps in Figure 5A show the classic alpha lateralization pattern for the instructed condition but not the willed condition. At 1190 ms post cue alpha topographic maps in Figure 5B, the opposite is observed.

Table 1. Timing of EEG events from UF and UCD datasets

EEG measures	UF dataset (ms)	UCD dataset (ms)
Willed theta onset	470	510
Willed theta offset	690	850
Instructed ALI onset	730	710
Willed ALI onset	1190	1010

ALI, alpha lateralization index.

Neural Substrate of Frontal Theta Activity

The possible neuroanatomical substrate of the frontal theta activity was examined by correlating trial-by-trial cue evoked frontal theta power during the time period of interest (400–800 ms) with the corresponding cue evoked BOLD activity using a parametric regressor technique (see Materials and Methods). Combining the trials from instructed and willed conditions, we found that frontal theta was most positively correlated with middle/dorsal anterior cingulate region (MCC)/dACC region (Fig. 6), and most negatively correlated with the posterior cingulate cortex (PCC) of the default mode network (Fig. 6). The coordinates for all the regions positively and negatively correlated with frontal theta are listed in Table 2.

UCD Dataset

The replicability of the foregoing findings from the UF dataset was tested by applying the same analytic strategy to the UCD dataset. Consistent with the results from the UF dataset, at the behavioral level, there was no significant difference in RT or accuracy between willed and instructed conditions. For the fMRI data, the DAN, including FEF and IPS, was similarly activated by both instruction and willed cues, and the contrast between willed and instructional cues showed a similar set of frontal parietal regions that were more activated for willed attention, including bilateral DLPFC, insula, dACC, APFC, SFG, IPL (see Liu et al. 2017 for more details). That covert attention was sustained during the cue-target interval was supported by ERP analysis showing that the N1 amplitude for attended targets was higher than the unattended targets (Bengson et al. 2014).

For EEG oscillatory activities, as shown in Supplementary Figures S1–S3, the difference spectrogram for the frontal ROI contrasting the willed condition and the instructed condition revealed a pattern similar to the UF pattern, where the onset and offset of theta power increase was 510 and 850 ms post cue; the same quantities determined from the UF dataset were 470 and 690 ms post cue (Table 1 and Supplementary Fig. S1). There was a significant increase in the frontal theta power for the willed condition as compared with the instructed condition (Table 3 and Supplementary Fig. S1). The functional connectivity between the frontal and parietal ROIs in the theta band

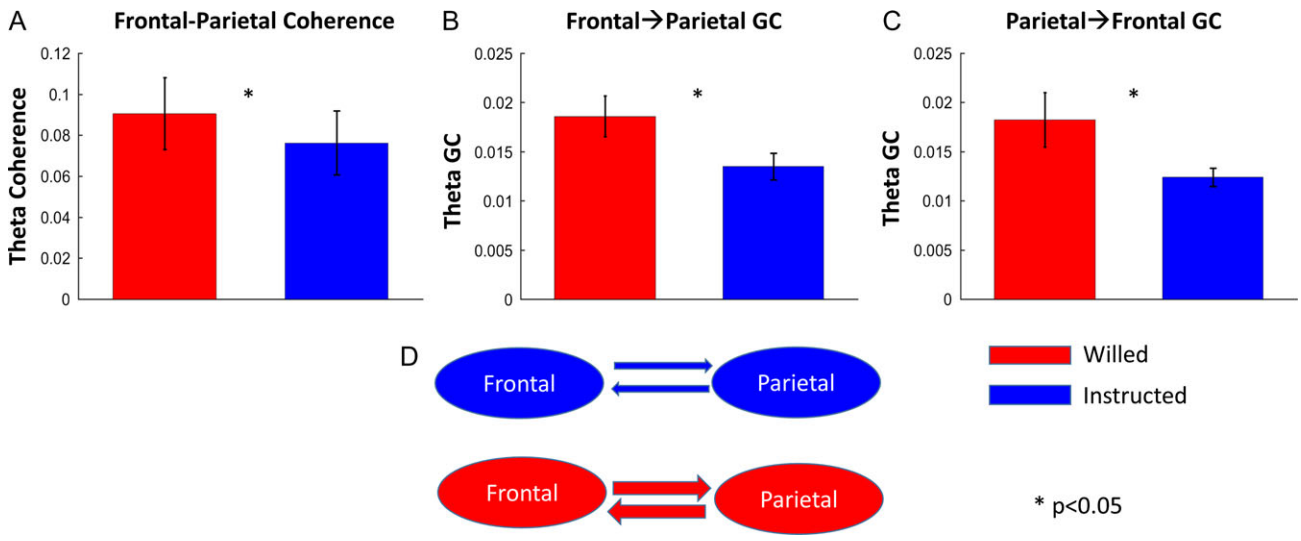

Figure 4. Frontal–parietal theta connectivity (400–800 ms). (A) Bar plot showing significantly higher frontal–parietal theta coherence for choice cues as compared with instruction cues. (B, C) Bar plots showing a significant higher bidirectional Granger causality (GC) for choice cues. (D) A schematic diagram of the GC result.

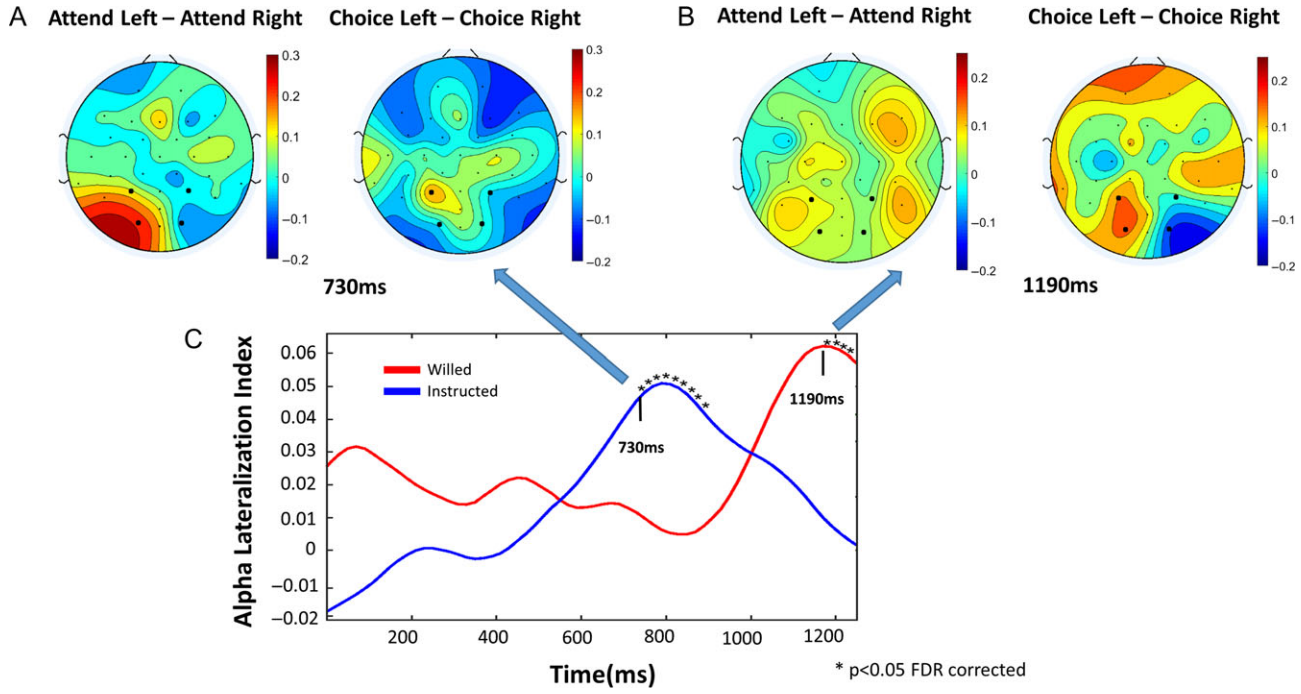

Figure 5. Time course of alpha (8–12 Hz) lateralization. (*A*) At 730 ms post cue, the instructed condition shows the classical pattern of alpha lateralization towards the attended hemifield, but this pattern is absent in the willed condition. (*B*) At 1190 ms post cue, the willed condition shows the classical pattern of alpha lateralization towards the chosen hemifield of attentional focus; this pattern is no longer apparent in the instructed condition. (*C*) Time course of alpha lateralization index (ALI) in response to willed and instructional cues.

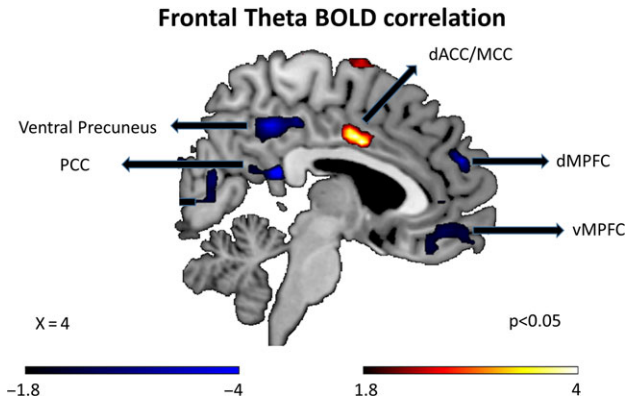

Figure 6. Regions showing positive and negative BOLD correlation with frontal theta power using EEG-informed fMRI analysis. dACC, dorsal anterior cingulate cortex; dMPFC, dorsal medial prefrontal cortex; MCC, middle cingulate cortex; PCC, posterior cingulate cortex.

showed a significant increase in coherence and bidirectional Granger causality, frontal→parietal and parietal→frontal, in the theta-band for the willed condition as compared with the instructed condition (Table 3 and Fig. S2). The attention allocation onset time from the ALI time course analysis was found to be 710 ms post cue for the instructed condition and 1010 ms post cue for the willed condition; the attention allocation onset times for the UF dataset for the same 2 conditions were 730 and 1190 ms (Table 1 and Supplementary Fig. S3).

Table 2. Regions showing positive and negative correlations between BOLD and frontal theta (UF data) ($P < 0.05$)

Anatomical region	MNI coordinates	*T*-value
Positively correlated with frontal theta		
dACC/MCC	3,3,33	4.85
Right precentral/MFG	39,−6,60	4.27
lSSC	−21,−36,75	3.19
lSPL	−30,−60,51	3.19
rSTG	66,−15,12	3.73
rAPFC	15,30,63	2.51
Negatively correlated with frontal theta		
PCC	3,−39,18	−7.05
Right lingual gyrus	15,−81,−12	−7.05
lSFG	−12, 21,57	−5.59
rOFC	51,36,−12	−4.59
dMPFC	12,45,39	−4.09
vMPFC	12,45,−12	−3.95
Left lingual gyrus	−15,−93,−12	−3.86
Left precuneus	−9,−69,48	−3.67
rMTG	69,−39,9	−3.35

dACC, dorsal anterior cingulate cortex; MCC, middle cingulate cortex; MFG, middle frontal gyrus; lSSC, left somatosensory cortex; lSPL, left superior parietal lobule; rSTG, right superior temporal gyrus; rAPFC, right anterior prefrontal cortex; PCC, posterior cingulate cortex; lSFG, left superior frontal gyrus; rOFC, right orbitofrontal cortex; dMPFC, dorsal medial prefrontal cortex; vMPFC, ventral medial prefrontal cortex; rMTG, right middle temporal gyrus.

Discussion

The neural underpinnings of willed attention were investigated by analyzing 2 EEG and fMRI datasets recorded at 2 different institutions using the same paradigm. We found that: 1) the DAN was activated by both the instructional cues and the choice cues, and additional brain regions such as DLPFC and dACC were preferentially activated by the choice cues (willed attention); these findings have been reported in our previous

Table 3. EEG theta-band spectral analysis results from UCD and UF dataset

EEG measures (theta band)	UCD data		Willed> instructed	UF data		Willed> instructed
	Willed attention	Instructed attention		Willed attention	Instructed attention	
Frontal power	0.340 ± 0.24	0.230 ± 0.19	$P < 0.05$	0.300 ± 0.259	0.117 ± 0.159	$P < 0.05$
F–P coherence	0.030 ± 0.015	0.023 ± 0.017	$P < 0.005$	0.091 ± 0.064	0.077 ± 0.057	$P < 0.05$
F→P GC	0.011 ± 0.004	0.006 ± 0.004	$P < 0.001$	0.019 ± 0.008	0.014 ± 0.005	$P < 0.05$
P→F GC	0.010 ± 0.005	0.006 ± 0.003	$P < 0.001$	0.018 ± 0.010	0.012 ± 0.003	$P < 0.05$

F, frontal; P, parietal; GC, Granger causality.

publications but were included here for completeness and self-containedness (Bengson et al. 2015; Liu et al. 2017); 2) frontal theta power, an index of decision-making and conflict resolution, was significantly higher for willed attention relative to instructed attention, and the frontoparietal coherence and frontal→parietal and parietal→frontal Granger causality in the theta band was also significantly higher for the willed condition, suggesting that theta mediates reciprocal frontal–parietal communications during decision making and subsequent attention deployment; and 3) as a consequence of increased processing time of the choice cue, the implementation of the posterior attention set (indexed by the onset of alpha lateralization) was delayed in willed condition by approximately 400–500 ms. Importantly, the above results are found to be consistent across the 2 datasets, demonstrating the reproducibility of the findings. For the UF dataset, where EEG and fMRI were recorded simultaneously, an EEG informed fMRI analysis further revealed that the trial-by-trial fluctuations of the frontal theta power is positively correlated with the BOLD fluctuations in the dACC region and negatively correlated with the BOLD fluctuations in the default mode network, suggesting a possible neuroanatomical correlate of, and perhaps generator/modulator of, the frontal theta activity in the present paradigm.

In willed attention, the choice cue evokes a cascade of events including conflict resolution, decision-making, and implementation of the attention set. The frontal theta has long been associated with conflict processing and decision-making. In particular, theta has been suggested to act as an "alarm signal," signaling the need to involve more cognitive control (Cavanagh and Frank 2014). In line with this, higher conflict situations are found to be accompanied by higher frontal theta (Cohen and Donner 2013; Cohen and Ridderinkhof 2013; Pastötter et al. 2013). Further, frontal theta has been shown to be involved in various aspects of decision-making. For example, frontal theta is involved in risk evaluation (Pinner and Cavanagh 2017), postdecision error monitoring (Cavanagh et al. 2010), and uncertainty evaluation (Cavanagh et al. 2012). These studies support the interpretation that the observed frontal theta increase represents the conflict resolution and decision-making aspects of willed attention; such theta activity is largely absent in instructed attention. Furthermore, our current results provide evidence for the involvement of frontal theta in free choice-based decisions, namely, decisions not associated with any specific rewards or risks.

It is known that frontal theta can increase in response to rare task-relevant stimuli such as the oddball stimuli in p300 paradigms (Mazaheri and Picton 2005). In our task, although the probability of attend-left cue, attend-right cue, and choice cue is equated, semantically, choice cues are rarer than instruction cues when attend-left cues and attend-right cues are combined (1/3 versus 2/3). We argue that the reported frontal theta increase following choice cues is unlikely to be rarity related based on timing information. The peak power of rarity-related frontal theta occurs around ~300 ms post stimulus, which is more than 200 ms earlier than the peak power of frontal theta observed here, which is 550–600 ms in both UF and UCD datasets (Mazaheri and Picton 2005; Ko et al. 2012; Hajihosseini and Holroyd 2013). Bengson et al. (2015) suggested that stimulus rarity was reflected in an ERP component, called Early Willed Attention Component (EWAC), which occurred in the time period 250–350 ms post cue. In the same study, a Willed Attention Component (WAC), occurring in the time period 400–800 ms post cue, was also identified and thought to be related to the decisional processing of willed attention. The timing of ERP WAC coincides with that of theta increase reported here, and together, they capture both the phase-locked and oscillatory aspects of decisional making/conflict processing in willed attention. Further experimentation examining the factors contributing to the timing of decision-making and conflict-processing related frontal theta increase is currently underway.

Frontal brain regions such as dACC and DLPFC are involved in both decision-making and conflict resolution (Kim and Shadlen 1999; Botvinick et al. 2001; Cavanagh et al. 2009). It remains unclear, however, the extent to which frontal theta reflects activity in these higher-order brain regions. To examine this, EEG informed fMRI analysis was conducted for the UF dataset where EEG and fMRI are simultaneously recorded. The positive correlation between BOLD activity in dACC region and frontal theta is in line with growing evidence suggesting dACC as the putative source for frontal theta (Onton et al. 2005; Tsujimoto et al. 2006; Hsieh and Ranganath 2014). More importantly, higher activity in dACC has been widely associated with detection of conflict and its resolution (Botvinick et al. 2004); thus, positive correlation with frontal theta further strengthens the idea that theta power is a neural marker for the conflict processing inherent in willed attention. The inverse correlation between frontal theta power and BOLD in the default mode network is expected due to deactivation of DMN in tasks requiring externally directed attention (Wen et al. 2013). Past work has also shown that even during rest the inverse relationship between DMN activity and frontal theta is preserved (Scheeringa et al. 2008).

Volitional acts involve complex cognitive operations and require communication between frontal and parietal regions (Haggard 2005, 2008). For instance, movement decisions such as choosing between different saccades or reaching goals can activate a premotor–parietal circuit (Haggard 2008). Invasive recordings from monkeys have shown that the act of freely choosing between different movement alternatives can activate

a frontal–parietal decision circuit to implement cognitive control mechanisms (Pesaran et al. 2008). In such movement-based choice making, frontal regions would need to make the choice and communicate the decision to parietal cortex, which then forms specific motor plans to execute the action (Mazzoni et al. 1996; Cui and Andersen 2007). In spatial attention, in addition to the frontal involvement in decision-making and conflict resolution discussed in the foregoing, the role of the posterior parietal regions in implementing the attentional set and issuing top-down signals to bias sensory processing is well-established (Hopfinger et al. 2000; Corbetta and Shulman 2002; Han et al. 2004). In agreement with these ideas, the graph-theoretic analysis by Liu et al. (2017) on fMRI BOLD signals suggests that frontal–parietal interaction is an integral part of the neural processes underlying willed attention. The neural signals and the time course underlying these interactions are, however, beyond the ability of fMRI to address and constitute the main focus of this study.

Research in the past has found that theta oscillations serve as the signal that links frontal and parietal structures in a number of paradigms including working memory and attention (Sauseng et al. 2005, 2008). Moreover, low frequency oscillations such as theta are thought to be more suited for long-range communications (von Stein and Sarnthein 2000; Wang et al. 2012; Solomon et al. 2017), because slow oscillations have long time windows which allows distant neuronal assemblies to phase synchronize with each other (Fries 2005). In line with these considerations, we observed increased frontal–parietal theta coherence during willed attention. Further, the Granger causality analysis showed that this frontal–parietal communication is reciprocal in nature. Higher frontal → parietal Granger causality in willed attention may signify the need to communicate the attentional choice from the frontal executive regions to the parietal attention control regions. Higher parietal → frontal Granger causality in willed attention, in contrast, may suggest that the parietal attentional control regions also sends information to the frontal executive structures to fulfill their monitoring function. Evidence for such posterior to frontal communication has been demonstrated in Bengson et al. (2014) showing that decisions about where to attend during willed attention is influenced by the momentary patterns of brain activity in posterior brain regions before the onset of cue. Our GC finding suggests that such posterior to frontal communication continues to occur during the post cue period when attentional decisions are being implemented in posterior cortex.

For instructed attention, the implementation of the attentional set is directly triggered by the instructional cues, which require minimal involvement of prefrontal resources outside those engaged as part of the DAN. For willed attention, in contrast, one might posit that extra processing time is required for the cognitive processes associated with the choice cue to resolve themselves, which would predict a delay in the implementation of attentional set in posterior brain regions. To test this idea, alpha lateralization, a reliable indicator of sensory biasing controlled by the DAN (Liu et al. 2016; Wang et al. 2016), was computed using a moving window approach. The analysis revealed that the onset of alpha lateralization is significantly delayed in willed versus instructed attention and the amount of delay (400–500 ms) may be taken as a measure of the time it takes for resolving conflicts and completing the decision-making in frontal structures. It is worth noting that this time period is longer than the previous estimates of conflict processing and resolution. For instance, in the Stroop task, conflict processing, measured as the difference in the RT to incongruent relative to congruent stimuli, involves time in the range of 200 ms (Kane and Engle 2003; Wang et al. 2015). Such conflict related processing, however, does not engage the process of willful decision making which could account for the extra time delay during willed attention.

In conclusion, the current study provided a novel and replicable view of the neural mechanisms of willed attention by analyzing the datasets recorded independently at 2 sites using the same paradigm. Consistent across the 2 datasets, the results demonstrated a role of theta oscillations in indexing frontal conflict resolution and decision-making as well as in mediating the reciprocal communications between frontal executive structures and parietal attention control regions during willed attention. Furthermore, our theta time–frequency and alpha lateralization time course analysis helped to elucidate the temporal dynamics of willed attention, complementing fMRI analysis. Finally, using the simultaneous EEG–fMRI technology, we provided evidence for dACC and default mode network as being possible neuroanatomical substrate of frontal theta oscillations in willed attention.

Supplementary Material

Supplementary material is available at *Cerebral Cortex* online.

Funding

National Institutes of Health grant R01-MH55714 (G.R.M.) and National Science Foundation grant BCS-1439188 (M.D.).

Notes

Conflict of Interest: None declared.

References

Allen PJ, Josephs O, Turner R. 2000. A method for removing imaging artifact from continuous EEG recorded during functional MRI. Neuroimage. 12:230–239.

Allen PJ, Polizzi G, Krakow K, Fish DR, Lemieux L. 1998. Identification of EEG events in the MR scanner: the problem of pulse artifact and a method for its subtraction. Neuroimage. 8:229–239.

Bengson JJ, Kelley TA, Mangun GR. 2015. The neural correlates of volitional attention: a combined fMRI and ERP study. Hum Brain Mapp. 36:2443–2454.

Bengson JJ, Kelley TA, Zhang X, Wang J-L, Mangun GR. 2014. Spontaneous neural fluctuations predict decisions to attend. J Cogn Neurosci. 26:2578–2584.

Botvinick MM, Braver TS, Barch DM, Carter CS, Cohen JD. 2001. Conflict monitoring and cognitive control. Psychol Rev. 108: 624–652.

Botvinick MM, Cohen JD, Carter CS. 2004. Conflict monitoring and anterior cingulate cortex: an update. Trends Cogn Sci. 8: 539–546.

Bressler SL, Tang W, Sylvester CM, Shulman GL, Corbetta M. 2008. Top-down control of human visual cortex by frontal and parietal cortex in anticipatory visual spatial attention. J Neurosci. 28:10056–10061.

Büchel C, Holmes AP, Rees G, Friston KJ. 1998. Characterizing stimulus-response functions using nonlinear regressors in parametric fMRI experiments. Neuroimage. 8:140–148.

Carrasco M. 2011. Visual attention: the past 25 years. Vision Res. 51:1484–1525.

Cavanagh JF, Cohen MX, Allen JJB. 2009. Prelude to and resolution of an error: EEG phase synchrony reveals cognitive control dynamics during action monitoring. J Neurosci. 29: 98–105.

Cavanagh JF, Frank MJ, Klein TJ, Allen JJB. 2010. Frontal theta links prediction errors to behavioral adaptation in reinforcement learning. Neuroimage. 49:3198–3209.

Cavanagh JF, Figueroa CM, Cohen MX, Frank MJ. 2012. Frontal theta reflects uncertainty and unexpectedness during exploration and exploitation. Cereb Cortex. 22:2575–2586.

Cavanagh JF, Frank MJ. 2014. Frontal theta as a mechanism for cognitive control. Trends Cogn Sci. 18:414–421.

Cohen MX. 2014. A neural microcircuit for cognitive conflict detection and signaling. Trends Neurosci. 37:480–490.

Cohen MX, Donner TH. 2013. Midfrontal conflict-related theta-band power reflects neural oscillations that predict behavior. J Neurophysiol. 110:2752–2763.

Cohen MX, Ridderinkhof KR. 2013. EEG source reconstruction reveals frontal-parietal dynamics of spatial conflict processing. PLoS One. 8:e57293.

Corbetta M, Shulman GL. 2002. Control of goal-directed and stimulus-driven attention in the brain. Nat Rev Neurosci. 3: 201–215.

Cui H, Andersen RA. 2007. Posterior parietal cortex encodes autonomously selected motor plans. Neuron. 56:552–559.

Dhamala M, Rangarajan G, Ding M. 2008. Analyzing information flow in brain networks with nonparametric Granger causality. Neuroimage. 41:354–362.

Ertl M, Kirsch V, Leicht G, Karch S, Olbrich S, Reiser M, Hegerl U, Pogarell O, Mulert C. 2010. Avoiding the ballistocardiogram (BCG) artifact of EEG data acquired simultaneously with fMRI by pulse-triggered presentation of stimuli. J Neurosci Methods. 186:231–241.

Foster JJ, Sutterer DW, Serences JT, Vogel EK, Awh E. 2017. Alpha-band oscillations enable spatially and temporally resolved tracking of covert spatial attention. Psychol Sci. 28: 929–941.

Fries P. 2005. A mechanism for cognitive dynamics: neuronal communication through neuronal coherence. Trends Cogn Sci. 9:474–480.

Giesbrecht B, Woldorff MG, Song AW, Mangun GR. 2003. Neural mechanisms of top-down control during spatial and feature attention. Neuroimage. 19:496–512.

Gulbinaite R, van Rijn H, Cohen MX. 2014. Fronto-parietal network oscillations reveal relationship between working memory capacity and cognitive control. Front Hum Neurosci. 8: 761.

Haggard P. 2005. Conscious intention and motor cognition. Trends Cogn Sci. 9:290–295.

Haggard P. 2008. Human volition: towards a neuroscience of will. Nat Rev Neurosci. 9:934–946.

Hajihosseini A, Holroyd CB. 2013. Frontal midline theta and N200 amplitude reflect complementary information about expectancy and outcome evaluation. Psychophysiology. 50: 550–562.

Han S, Jiang Y, Gu H, Rao H, Mao L, Cui Y, Zhai R. 2004. The role of human parietal cortex in attention networks. Brain. 127: 650–659.

Handy TC, Mangun GR. 2000. Attention and spatial selection: electrophysiological evidence for modulation by perceptual load. Percept Psychophys. 62:175–186.

Heekeren HR, Marrett S, Ungerleider LG. 2008. The neural systems that mediate human perceptual decision making. Nat Rev Neurosci. 9:467–479.

Heinze HJ, Mangun GR, Burchert W, Hinrichs H, Scholz M, Münte TF, Gös A, Scherg M, Johannes S, Hundeshagen H, et al. 1994. Combined spatial and temporal imaging of brain activity during visual selective attention in humans. Nature. 372:543.

Hopfinger JB, Buonocore MH, Mangun GR. 2000. The neural mechanisms of top-down attentional control. Nat Neurosci. 3:284–291.

Hsieh L-T, Ranganath C. 2014. Frontal midline theta oscillations during working memory maintenance and episodic encoding and retrieval. Neuroimage. 85:721–729.

Kalcher J, Pfurtscheller G. 1995. Discrimination between phase-locked and non-phase-locked event-related EEG activity. Electroencephalogr Clin Neurophysiol. 94:381–384.

Kane MJ, Engle RW. 2003. Working-memory capacity and the control of attention: the contributions of goal neglect, response competition, and task set to Stroop interference. J Exp Psychol Gen. 132:47–70.

Kastner S, Pinsk MA, De Weerd P, Desimone R, Ungerleider LG. 1999. Increased activity in human visual cortex during directed attention in the absence of visual stimulation. Neuron. 22:751–761.

Kim JN, Shadlen MN. 1999. Neural correlates of a decision in the dorsolateral prefrontal cortex of the macaque. Nat Neurosci. 2:176–185.

Ko D, Kwon S, Lee G-T, Im CH, Kim KH, Jung K-Y. 2012. Theta oscillation related to the auditory discrimination process in mismatch negativity: oddball versus control paradigm. J Clin Neurol. 8:35–42.

Lau HC, Rogers RD, Ramnani N, Passingham RE. 2004. Willed action and attention to the selection of action. Neuroimage. 21:1407–1415.

Liu Y, Bengson J, Huang H, Mangun GR, Ding M. 2016. Top-down modulation of neural activity in anticipatory visual attention: control mechanisms revealed by simultaneous EEG-fMRI. Cereb Cortex. 26:517–529.

Liu Y, Hong X, Bengson JJ, Kelley TA, Ding M, Mangun GR. 2017. Deciding where to attend: large-scale network mechanisms underlying attention and intention revealed by graph-theoretic analysis. Neuroimage. 157:45–60.

Mangun GR, Hillyard SA. 1991. Modulations of sensory-evoked brain potentials indicate changes in perceptual processing during visual-spatial priming. J Exp Psychol Hum Percept Perform. 17:1057–1074.

Maris E, Oostenveld R. 2007. Nonparametric statistical testing of EEG- and MEG-data. J Neurosci Methods. 164:177–190.

Mazzoni P, Bracewell RM, Barash S, Andersen RA. 1996. Motor intention activity in the macaque's lateral intraparietal area. I. Dissociation of motor plan from sensory memory. J Neurophysiol. 76:1439–1456.

Mazaheri A, Picton TW. 2005. EEG spectral dynamics during discrimination of auditory and visual targets. Cogn Brain Res. 24:81–96.

Moran J, Desimone R. 1985. Selective attention gates visual processing in the extrastriate cortex. Science. 229:782–784.

Nedungadi AG, Rangarajan G, Jain N, Ding M. 2009. Analyzing multiple spike trains with nonparametric Granger causality. J Comput Neurosci. 27:55–64.

Onton J, Delorme A, Makeig S. 2005. Frontal midline EEG dynamics during working memory. Neuroimage. 27:341–356.

Pastötter B, Dreisbach G, Bäuml K-HT. 2013. Dynamic adjustments of cognitive control: oscillatory correlates of the conflict adaptation effect. J Cogn Neurosci. 25:2167–2178.

Pesaran B, Nelson MJ, Andersen RA. 2008. Free choice activates a decision circuit between frontal and parietal cortex. Nature. 453:406–409.

Pinner JFL, Cavanagh JF. 2017. Frontal theta accounts for individual differences in the cost of conflict on decision making. Brain Res. 1672:73–80.

Posner M. 1978. Chronometric explorations of mind. New York: Oxford University Press.

Posner MI. 1980. Orienting of attention. Q J Exp Psychol. 32:3–25.

Rajagovindan R, Ding M. 2011. From prestimulus alpha oscillation to visual-evoked response: an inverted-U function and its attentional modulation. J Cogn Neurosci. 23:1379–1394.

Reynolds JH, Chelazzi L. 2004. Attentional modulation of visual processing. Annu Rev Neurosci. 27:611–647.

Sauseng P, Klimesch W, Gruber WR, Birbaumer N. 2008. Cross-frequency phase synchronization: a brain mechanism of memory matching and attention. Neuroimage. 40:308–317.

Sauseng P, Klimesch W, Schabus M, Doppelmayr M. 2005. Fronto-parietal EEG coherence in theta and upper alpha reflect central executive functions of working memory. Int J Psychophysiol. 57:97–103.

Scheeringa R, Bastiaansen MCM, Petersson KM, Oostenveld R, Norris DG, Hagoort P. 2008. Frontal theta EEG activity correlates negatively with the default mode network in resting state. Int J Psychophysiol. 67:242–251.

Solomon EA, Kragel JE, Sperling MR, Sharan A, Worrell G, Kucewicz M, Inman CS, Lega B, Davis KA, Stein JM, et al. 2017. Widespread theta synchrony and high-frequency desynchronization underlies enhanced cognition. Nat Commun. 8:1704.

Taylor PCJ, Rushworth MFS, Nobre AC. 2008. Choosing where to attend and the medial frontal cortex: an FMRI study. J Neurophysiol. 100:1397–1406.

Tenke CE, Kayser J. 2012. Generator localization by current source density (CSD): implications of volume conduction and field closure at intracranial and scalp resolutions. Clin Neurophysiol. 123:2328–2345.

Thut G, Nietzel A, Brandt SA, Pascual-Leone A. 2006. Alpha-band electroencephalographic activity over occipital cortex indexes visuospatial attention bias and predicts visual target detection. J Neurosci. 26:9494–9502.

Tootell RB, Hadjikhani N, Hall EK, Marrett S, Vanduffel W, Vaughan JT, Dale AM. 1998. The retinotopy of visual spatial attention. Neuron. 21:1409–1422.

Tsujimoto T, Shimazu H, Isomura Y. 2006. Direct recording of theta oscillations in primate prefrontal and anterior cingulate cortices. J Neurophysiol. 95:2987–3000.

von Stein A, Sarnthein J. 2000. Different frequencies for different scales of cortical integration: from local gamma to long range alpha/theta synchronization. Int J Psychophysiol. 38: 301–313.

Voorhis SV, Hillyard SA. 1977. Visual evoked potentials and selective attention to points in space. Percept Psychophys. 22:54–62.

Walsh BJ, Buonocore MH, Carter CS, Mangun GR. 2011. Integrating conflict detection and attentional control mechanisms. J Cogn Neurosci. 23:2211–2221.

Wang C, Ding M, Kluger BM. 2015. Functional roles of neural preparatory processes in a cued stroop task revealed by linking electrophysiology with behavioral performance. PLoS One. 10:e0134686.

Wang C, Rajagovindan R, Han S-M, Ding M. 2016. Top-down control of visual alpha oscillations: sources of control signals and their mechanisms of action. Front Hum Neurosci. 10:15.

Wang L, Saalmann YB, Pinsk MA, Arcaro MJ, Kastner S. 2012. Electrophysiological low-frequency coherence and cross-frequency coupling contributes to BOLD connectivity. Neuron. 76:1010–1020.

Wen X, Liu Y, Yao L, Ding M. 2013. Top-down regulation of default mode activity in spatial visual attention. J Neurosci. 33:6444–6453.

Wen X, Yao L, Liu Y, Ding M. 2012. Causal interactions in attention networks predict behavioral performance. J Neurosci. 32:1284–1292.

Worden MS, Foxe JJ, Wang N, Simpson GV. 2000. Anticipatory biasing of visuospatial attention indexed by retinotopically specific α-bank electroencephalography increases over occipital cortex. J Neurosci. 20:RC63–RC63.